Available online at www.sciencedirect.com
ScienceDirect
International Journal of Heat and Fluid Flow 29 (2008) 229–241
International Journal of HEAT AND FLUID FLOW
www.elsevier.com/locate/ijhff

Impacts of nanofluid flow on skin friction factor and Nusselt number in curved tubes with constant mass flow

A. Akbarinia *

New Energies Department, Energy Research Institute, International Center of Science, Technology & Environmental Science, Mahan, Iran

Received 15 January 2007; received in revised form 25 April 2007; accepted 8 May 2007
Available online 29 June 2007

Abstract

Three-dimensional elliptic governing equations were solved to investigate laminar mixed convection of a nanofluid consists of water and Al_2O_3, buoyancy-affected and heat transfer of a curved tube. Simultaneous effects of the buoyancy force, centrifugal force and nanoparticles concentration on the fluid flow developing and heat transfer along the pipe is investigated in this paper. The nanoparticles concentration does not have any significant effect on the secondary flow, while the axial velocity, Nusselt number, skin friction factor as well as fluid temperature have been affected considerably. In this paper, some important new results are obtained. Firstly, for a given flow rate; nanoparticles concentration have positive effects on the axial velocity and skin friction factor. Secondly, buoyancy force has negative effect on the Nusselt number and skin friction factor.

Keywords: Nanofluid; Curved pipe; Centrifugal force; Buoyancy force; Laminar mixed convection

1. Introduction

In order to cope with growing demand from different industries such as electronic, automotive and aerospace industries, heat exchanger devices have to be small in size, light in weight and of high performance. Low thermal conductivity of conventional heat transfer fluids such as water, oil, and ethylene glycol mixture is a serious limitation in improving the performance and compactness of these engineering equipments. To overcome those disadvantages, there is strong motivation to develop advanced heat transfer fluids with substantially higher conductivity. An innovative w ay of improving the thermal conductivities of fluids is to suspend small solid particles in the fluid. However, more than a century ago Maxwell (1873, 1904) showed the possibility of increasing thermal conductivity of a mixture by more volume fraction of solid particles.

Various types of powders such as metallic, non-metallic and polymeric particles can be added into fluids to form slurries. An industrial application test was carried out by Liu et al. (1988) and the effects of flow rates on the slurry pressure drop and heat transfer behavior was investigated. In conventional cases, the suspended particles are of μm or even mm in dimensions. However, such large particles may cause severe problems such as abrasion and clogging. Therefore, fluids with suspended large particles have little practical application in heat transfer enhancement.

Nanofluids are a new kind of heat transfer fluid containing a small quantity of nano-sized particles (usually less than 100 nm) that are uniformly and stably suspended in a liquid. The dispersion of a small amount of solid nanoparticles in conventional fluids changes their thermal conductivity remarkably. Compared to the existing techniques for enhancing heat transfer, the nanofluids show a superior potential for increasing heat transfer rates in a variety of cases. Choi (1995) quantitatively analyzed some potential benefits of nanofluids for augmenting heat transfer and reducing size, weight and cost of thermal apparatuses, while incurring little or no penalty in the pressure drop.

* Tel.: +98 9132993983; fax: +98 342622 6617.
E-mail address: akbarinia@icst.ac.ir

0142-727X/$ - see front matter © 2007 Elsevier Inc. All rights reserved.
doi:10.1016/j.ijheatfluidflow.2007.05.003

Nomenclature

a	radius of curved pipe (m)
C_p	specific heat (J/kg K)
d	horizontal direction
D	diameter of curved tube (m)
De	Dean number ($=Re.\delta^{1/2}$)
f_θ	local skin friction coefficient
g	gravitational acceleration (m s^{-2})
Gr	Grashof number $\left(=\frac{g\beta_{\text{eff}}q''D^4}{k_{\text{eff}}\upsilon_{\text{eff}}^2}\right)$
k	thermal conductivity (W/m K)
$\dot{m}$	flow rate ($=2\pi D\rho_{\text{eff}}u_0$)
Nu_θ	local Nusselt number $\left(=\frac{q''D}{k_{\text{eff}}(T_w-T_b)}\right)$
P	pressure (Pa)
Pr	Prandtl number $\left(=\frac{\alpha_{\text{eff}}}{\nu_{\text{eff}}}\right)$
q''	uniform heat flux (W m^{-2})
R_c	curvature radius
Re	Reynolds number $\left(=\frac{\rho_{\text{eff}}u_0D}{\mu_{\text{eff}}}\right)$
T	temperature (K)
u, v	velocity (m s^{-1})
y	vertical direction

Greeks

α	thermal diffusivity
β	volumetric expansion coefficient (K^{-1})
δ	curvature ratio ($=a/R_c$)
θ	angular coordinate in axial direction
ϕ	volume fraction
μ	dynamic viscosity (N s m^{-2})
ν	kinematics viscosity (m^2 s^{-1})
ρ	density (kg m^{-3})

Subscripts

b	bulk
eff	effective
f	base fluid
m	average
0	inlet condition
r	radial direction
w	wall
z	axial direction
φ	tangential direction

Researchers have demonstrated that oxide ceramic nanofluids consisting of CuO or Al_2O_3 nanoparticles in water or ethylene glycol exhibit enhanced thermal conductivity (Lee et al., 1999). A maximum increase in thermal conductivity of approximately 20% was observed in that study, having 4 vol.% CuO nanoparticles with mean diameter 35 nm dispersed in ethylene glycol. A similar behavior has been observed in Al_2O_3/water nanofluid. For example, using Al_2O_3 particles having a mean diameter of 13 nm at 4.3% volume fraction increased the thermal conductivity of water under stationary conditions by 30% (Masuda et al., 1993). On the other hand, larger particles with an average diameter of 40 nm led to an increase of less than 10% (Lee et al., 1999). Furthermore, the effective thermal conductivity of metallic nanofluid increased by up to 40% for the nanofluid consisting of ethylene glycol containing approximately 0.3 vol.% Cu nanoparticles of mean diameter less than 10 nm (Choi, 1995).

Different concepts have been proposed to explain this enhancement in heat transfer. Xuan and Li (2000) and Xuan and Roetzel (2000) have identified two causes of improved heat transfer by nanofluids: the increased thermal dispersion due to the chaotic movement of nanoparticles that accelerates energy exchanges in the fluid and the enhanced thermal conductivity of nanofluids considered by Choi (1995). On the other hand Keblinski et al. (2002) have studied four possible mechanisms that contribute to the increase in nanofluid heat transfer: Brownian motion of the particles, molecular-level layering of the liquid/particle interface, heat transport in the nanoparticles and nanoparticles clustering. Similarly to Wang et al. (1999), they showed that the effects of the interface layering of liquid

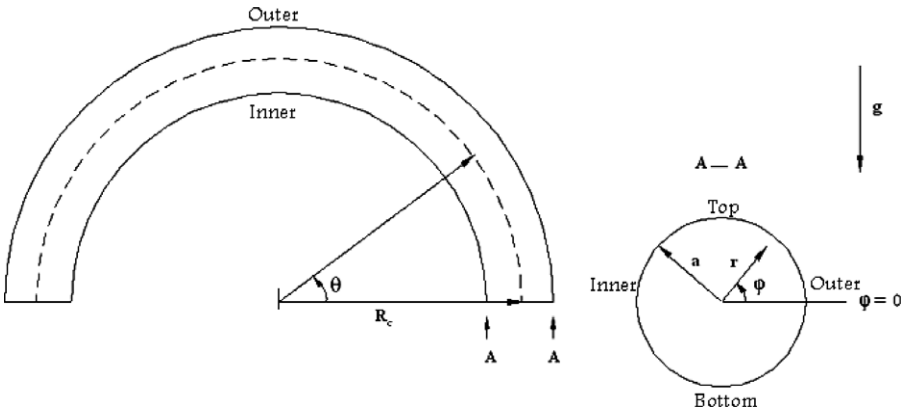

Fig. 1. Schematic of a horizontal curved tube.

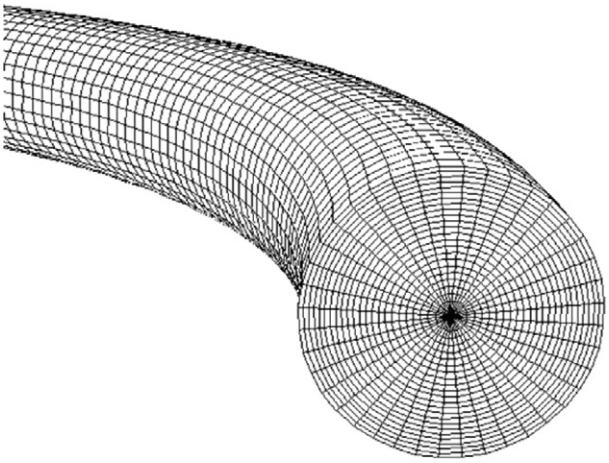

Fig. 2. Structured non-uniform grid of the curved tube.

molecules and nanoparticles clustering could provide paths for rapid heat transfer. Numerous theoretical and experimental studies have been conducted to determine the effective thermal conductivity of nanofluids. Most of these have been confined to liquids containing micro and milli-sized

Table 1
Grid independent test

Node number ($\varphi \times r \times z$)	Axial velocity (m/s)	Temperature (K)
$40 \times 60 \times 180$	0.076556	293.776
$52 \times 60 \times 180$	0.076548	293.773
$40 \times 40 \times 180$	0.076534	293.770
$40 \times 48 \times 180$	0.076555	293.773
$40 \times 72 \times 180$	0.076560	293.774
$40 \times 48 \times 130$	0.076624	293.771
$40 \times 48 \times 160$	0.076572	293.773

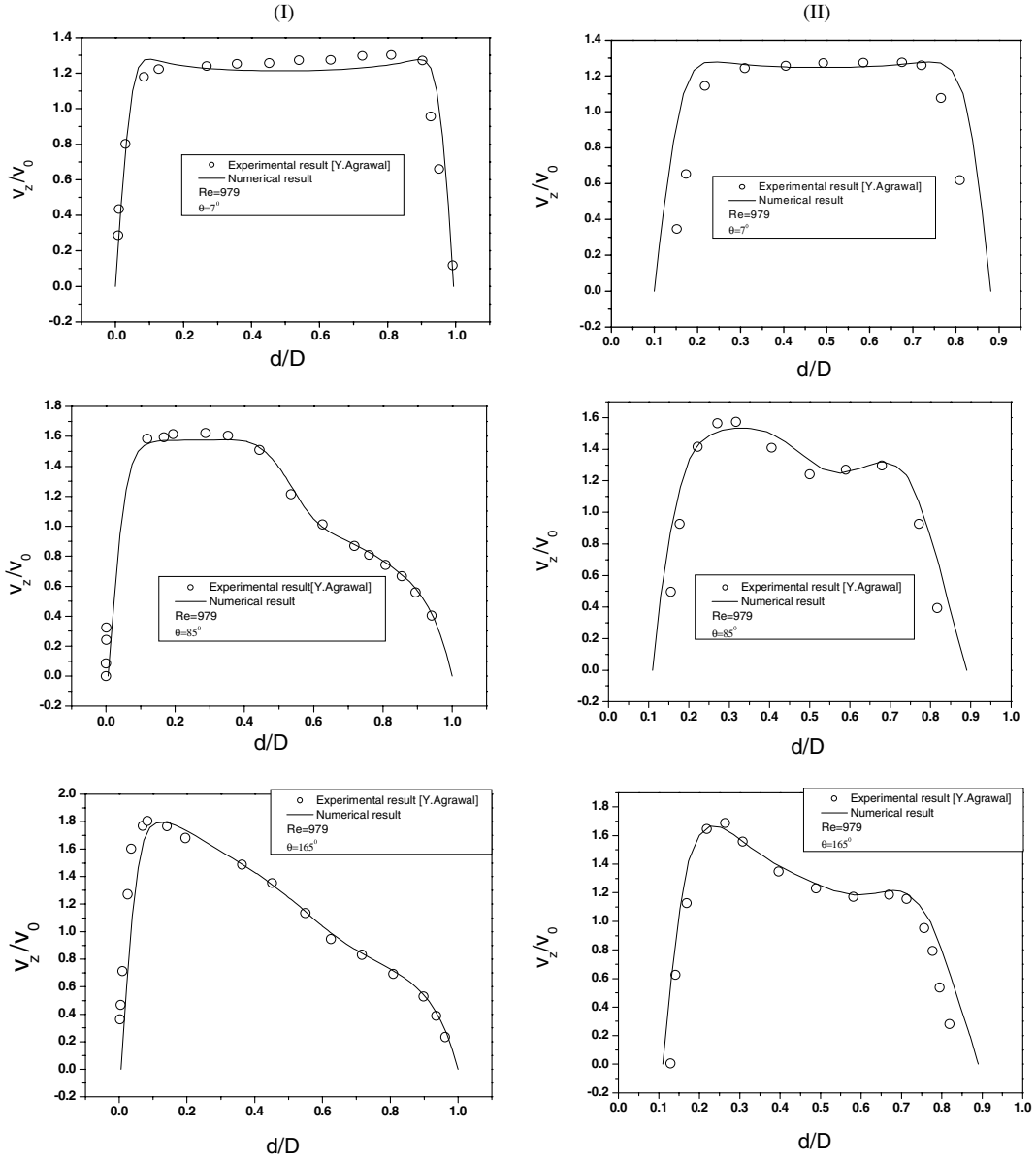

Fig. 3. Comparison of developing axial velocity profiles. (I) $\frac{\nu}{a} = -0.0668$ and (II) $\frac{\nu}{a} = -0.668$.

suspended solid particles. However, studies show that the measured thermal conductivity of nanofluids is much larger than the theoretical predictions (Choi et al., 2001). Many attempts have been made to formulate efficient theoretical models for the prediction of the effective thermal conductivity, but there is still a serious lack in this domain (Xue, 2003; Xuan et al., 2003).

As nanofluids are rather new, relatively few theoretical and experimental studies have been reported on convective heat transfer coefficients in confined flows. Pak and Cho (1998) and Xuan and Li (2000, 2003) obtained experimental results on convective heat transfer for laminar and turbulent flow of a nanofluid inside a tube. They produced the first empirical correlations for the Nusselt number using nanofluids composed of water and Cu, TiO_2 and Al_2O_3 nanoparticles. The results indicate a remarkable increase in heat transfer performance over the base fluid for the same Reynolds number.

Despite the fact that nanofluid is a two phase mixture, since the solid particles are very small size they are easily fluidized and can be approximately considered to behave as a fluid (Xuan and Li, 2000). Therefore, considering the

Table 2
Comparison of the calculated Nusselt number with pervious numerical data (Goering et al., 1997)

Gr		1000	3000	9700	29300	48,600	97,900	146,600
Present work	$\frac{Nu}{Nu_s}$	2.852953	2.85272	2.848779	2.8044276	2.7191752	2.58915	2.52724
Numerical Goering data		2.84543	2.84543	2.84543	2.77518	2.63466	2.42389	2.36534

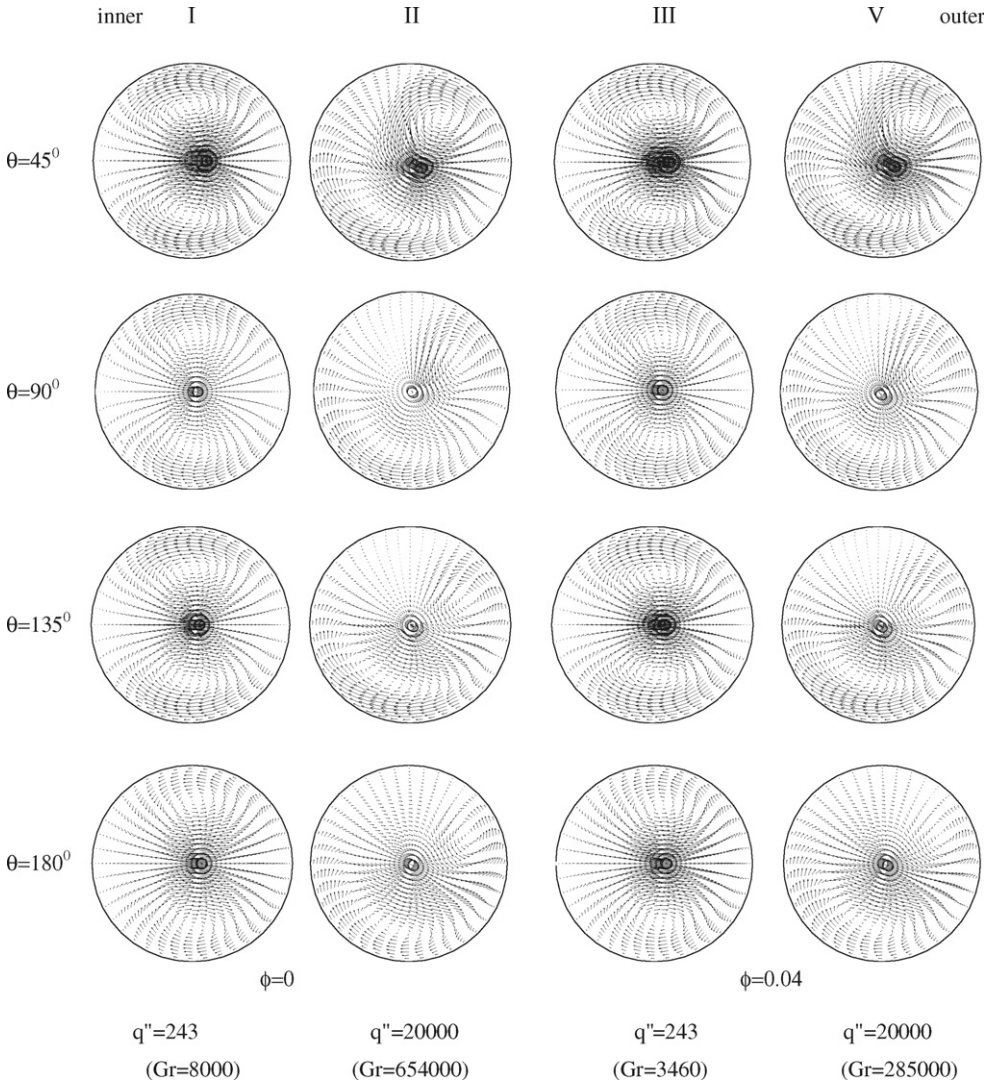

Fig. 4. Computed non-dimensional secondary flow at different axial position for $\dot{m} = 0.0024$ (kg/s).

ultrafine and low volume fraction of the solid particles, it might be reasonable to treat nanofluid as single phase flow in certain conditions (Yang et al., 2005).

The single phase approach assumes that the fluid phase and particles are in thermal equilibrium and move with the same velocity. This approach is simpler and requires less computational time. Thus it has been used in several theoretical studies of convective heat transfer with nanofluids (for example Maiga et al., 2004; Roy et al., 2004; Khanafer et al., 2003; Koo and Kleinstreuer, 2005). However, due to the fact that the effective properties of nanofluids are not known precisely, the numerical predictions of this approach are; in general, dependent on the considered effective physical properties.

Many researchers have become interested in mixed convection in a horizontal curved tube at the macro level (for instance Agrawal et al., 1978; Goering et al., 1997; Yang and Chang, 1994; Zheng et al., 2003). At such conditions buoyancy force and also the centrifugal force become important. Each of these forces could alone increase the Nusselt number. However, their simultaneous effects in the presence of the nanoparticles have not been studied.

The objective of the present paper is to study the effects of particles concentration on the hydrodynamic and thermal parameters of laminar mixed convection of a nanofluid in a horizontal curved tube at different mass flow rate and heat flux. Simultaneous effects of buoyancy force, centrifugal force and nanoparticles volume fraction in the base fluid on heat transfer augmentation are studied. Therefore, the axial velocity, secondary flow and temperature profiles for different values of the particles concentrations are presented at different axial angle and $\dot{m} - q''$ combinations. Also, the effects of nanoparticles concentration on peripheral Nusselt number and the peripheral skin friction at different q'' are shown and discussed.

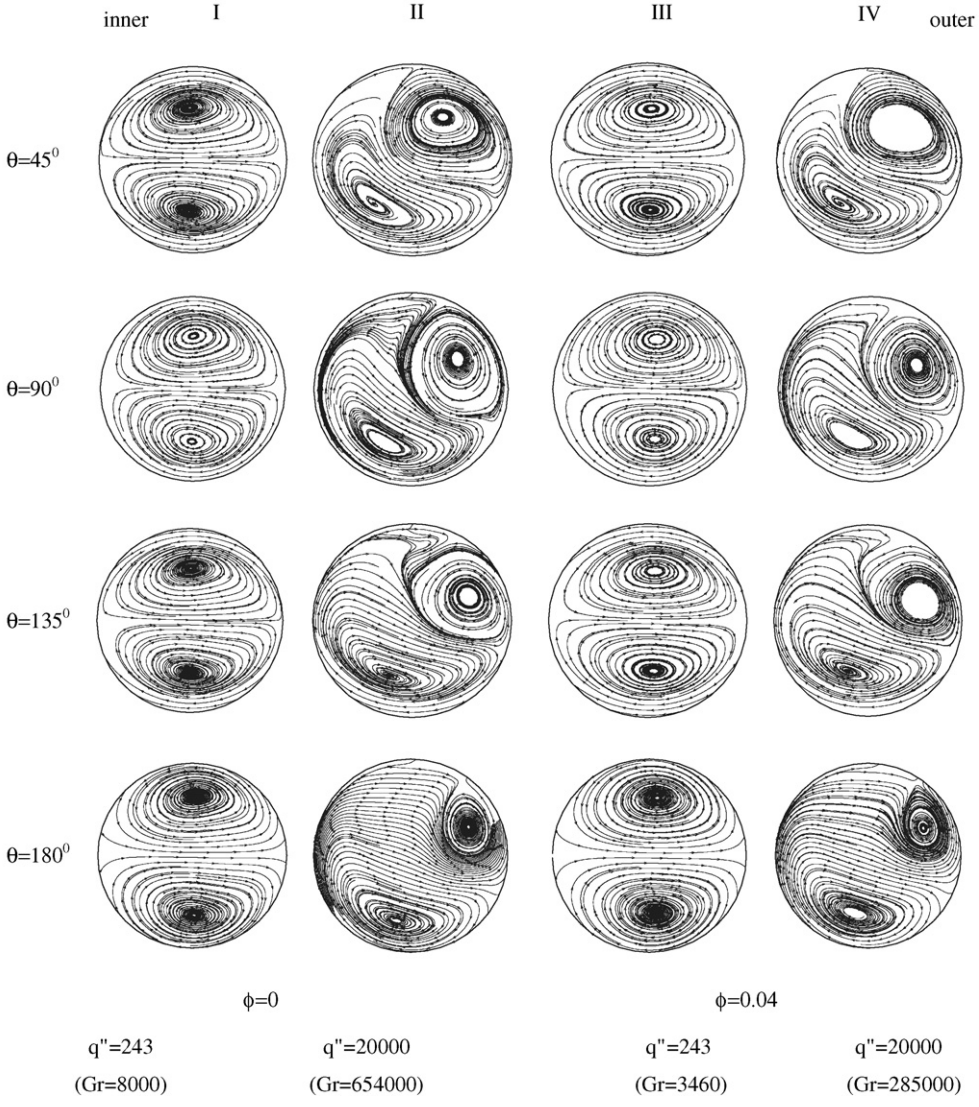

Fig. 5. Stream lines tracer for $\dot{m} = 0.0024$.

2. Mathematical modeling

2.1. Mathematical formulation and numerical procedure

Mixed convection of a nanofluid consists of water and Al_2O_3 in a horizontal curved tube with uniform heat flux at the solid–liquid interface has been considered. Fig. 1 shows the geometry of the considered problem. The computation domain is composed of a curved circular pipe where the axial angle θ ranges from 0° to 180° and with radius $a$and sectional angel φ Gravitational force is exerted in the vertical direction. The properties of the fluid are assumed constant except for the density in the body force, which varies linearly with the temperature (Boussinesq's hypothesis). Dissipation and pressure work are neglected. It is also assumed that the fluid phase and nanoparticles are in thermal equilibrium with zero relative velocity. With these assumptions the dimensional conservation equations for steady state mean conditions in the Cartesian coordinate are as follows:

Continuity:

$$\frac{\partial u_j}{\partial x_j} = 0 \tag{1}$$

Momentum:

$$\frac{\partial}{\partial x_j}(\rho_{\text{eff}} u_i u_j) = \frac{\partial}{\partial x_j}\left(\mu_{\text{eff}}\left(\frac{\partial u_i}{\partial x_j}\right)\right) - \frac{\partial p}{\partial x_i} - \rho_{\text{eff},0} g_i \beta_{\text{eff}}(T - T_0) \tag{2}$$

Energy:

$$\frac{\partial}{\partial x_i}[(\rho c_p)_{\text{eff}} u_i T] = \frac{\partial}{\partial x_i}\left(k_{\text{eff}} \frac{\partial T}{\partial x_i}\right) \tag{3}$$

where $i = 1, 2, 3$ and $u_i = (v_x, v_y, v_z)$ are velocity vectors.

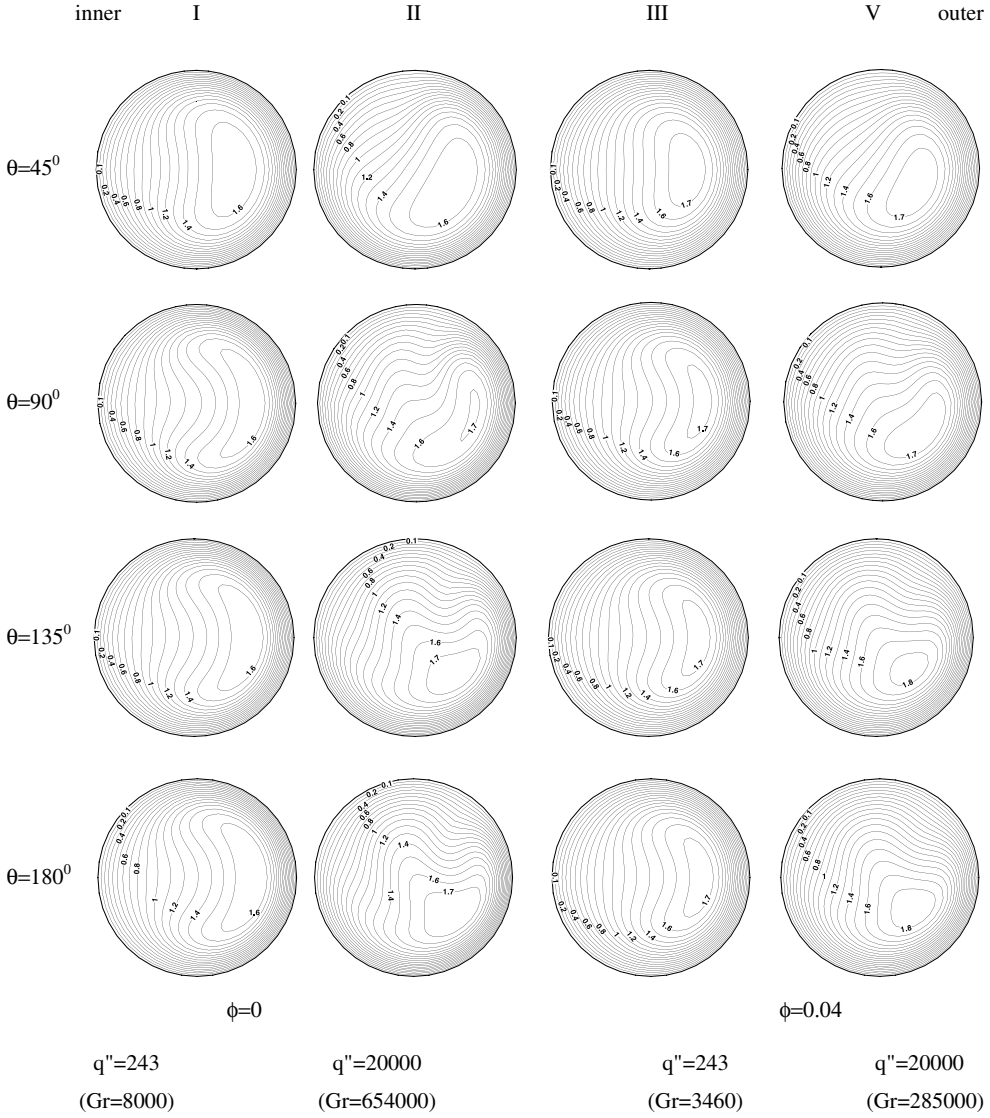

Fig. 6. Computed dimensionless iso-axial velocity contour at different axial position for $\dot{m} = 0.0024$ (kg/s).

2.2. Thermal and physical properties of nanofluids

The effective properties of the nanofluid (fluid containing suspended nanoparticles) are defined as follows:

Density:

$$\rho_{\mathrm{eff},0} = (1-\phi)\rho_{\mathrm{f},0} + \phi\rho_{\mathrm{s},0} \tag{4}$$

Viscosity:

$$\mu_{\mathrm{eff}} = (123\phi^2 + 7.3\phi + 1)\mu_{\mathrm{f}} \tag{5}$$

This was presented by Maiga et al. (2004) for water – Al_2O_3 nanofluid based on available experimental results in the literature.

Heat capacitance:

$$(c_p)_{\mathrm{eff}} = \left[\frac{(1-\phi)(\rho c_p)_{\mathrm{f}} + \phi(\rho c_p)_{\mathrm{s}}}{(1-\phi)\rho_{\mathrm{f}} + \phi\rho_{\mathrm{s}}}\right] \tag{6}$$

Effective thermal conductivity:

$$k_{\mathrm{eff}} = \left(\frac{k_{\mathrm{s}} + (n-1)k_{\mathrm{f}} - (n-1)\phi(k_{\mathrm{f}} - k_{\mathrm{s}})}{k_{\mathrm{s}} + (n-1)k_{\mathrm{f}} + \phi(k_{\mathrm{f}} - k_{\mathrm{s}})}\right)k_{\mathrm{f}} \tag{7}$$

This was introduced by Hamilton and Crosser (1962). Where n is a shape factor and is equal to 3 for spherical nanoparticles. This model appears appropriate for nanofluids (Xuan and Roetzel, 2000; Maiga et al., 2004; Roy et al., 2004; Palm et al., 2006; Zhang et al., 2006).

Thermal expansion coefficient:

$$\beta_{\mathrm{eff}} = \left[\frac{1}{1 + \frac{(1-\phi)\rho_{\mathrm{f}}}{\phi\rho_{\mathrm{s}}}}\frac{\beta_{\mathrm{s}}}{\beta_{\mathrm{f}}} + \frac{1}{1 + \frac{\phi}{1-\phi}\frac{\rho_{\mathrm{s}}}{\rho_{\mathrm{f}}}}\right]\cdot\beta_{\mathrm{f}} \tag{8}$$

This was presented and used by Khanafer et al. (2003).

Thermal diffusivity:

$$\alpha_{\mathrm{eff}} = \frac{k_{\mathrm{eff}}}{(1-\phi)(\rho c_p)_{\mathrm{f}} + \phi(\rho c_p)_{\mathrm{s}}} \tag{9}$$

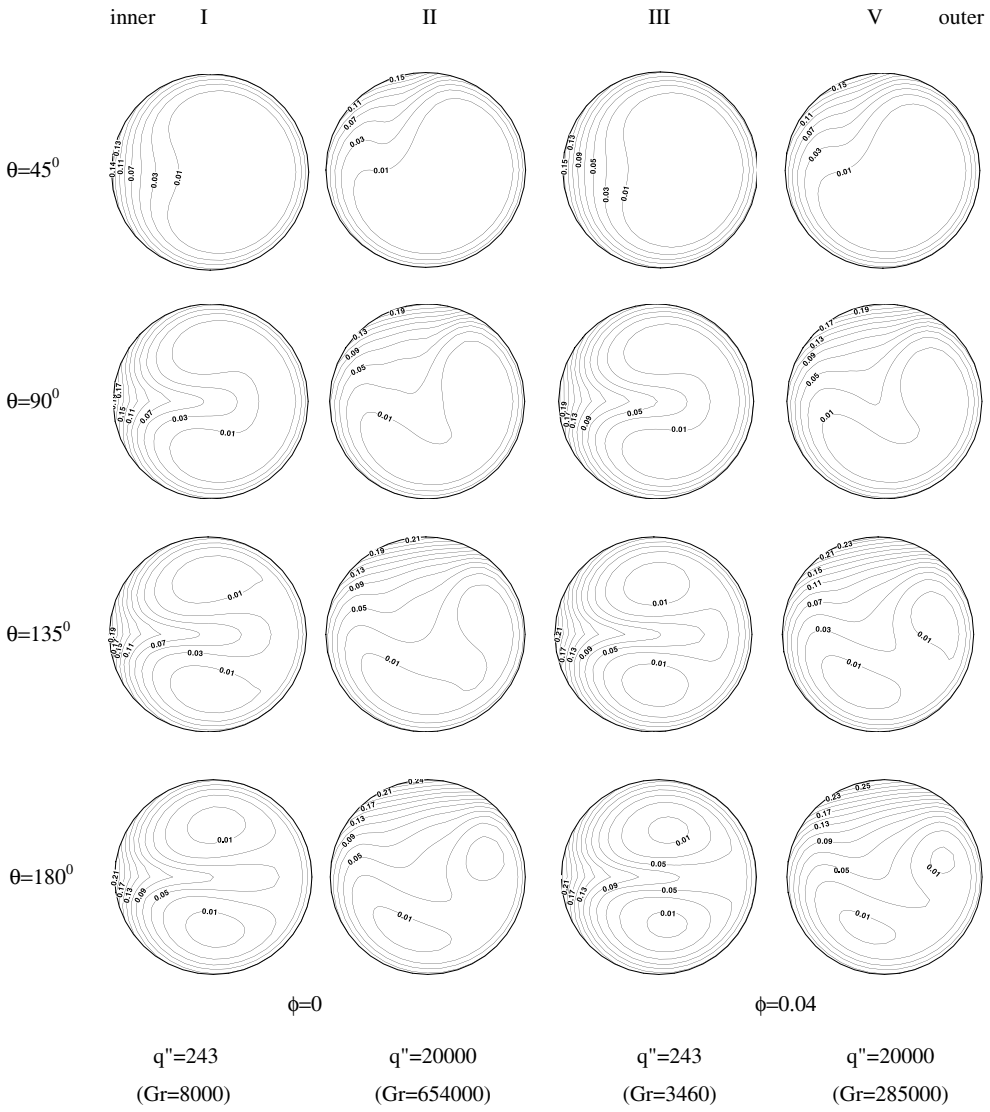

Fig. 7. Computed dimensionless iso-temperature contour at different axial position for $\dot{m} = 0.0024$ (kg/s).

2.3. Boundary condition

This set of non-linear elliptical governing equations has been solved subject to following boundary conditions:

- At the tube inlet $(\theta = 0)$: and $0 \leqslant r \leqslant a : v_r = 0;$ $v_\varphi = 0;\ v_z = v_0;\ T = T_0$ (10a)
- At the fluid–solid interface $(r = a) : v_r = v_\varphi = v_z = 0;$ $q_w = -k_{eff}\dfrac{\partial T}{\partial r}$ (10b)
- At the tube outlet $(\theta = 180)$ the diffusion flux in the direction normal to the exit plane is assumed to be zero for all variables and an overall mass balance correction is applied.

2.4. Numerical method and validation

The sets of coupled non-linear differential equations were discretized using the control volume technique. A second order upwind method was used for the convective and diffusive terms while the SIMPLEC procedure was introduced to couple the velocity–pressure. A structured non-uniform grid distribution has been used to discretize the computational domain as shown in Fig. 2. It is finer near the tube entrance and near the wall where the velocity and temperature gradients are large. Several different grid distributions have been tested to ensure that the calculated results are grid independent. The selected grid for the present calculations consisted of 160, 48 and 40 nodes in the axial, radial and circumferential directions respectively. As it shows in Table 1 increasing the grid numbers does not change significantly the velocity and temperature at the centerline region (see Table 1).

In order to demonstrate the validity and also precision of the model assumptions and the numerical analysis, calculated velocity at different axial positions is compared with the corresponding experimental results carried out by Agrawal et al. (1978) for water-glycerin at $Re = 979$. As it is shown in Fig. 3 a significant agreement between the numerical and experimental results are observed at different cross sections. On the other hand, calculated Nusselt number is compared with the corresponding numerical results carried out by Goering et al. (1997) for $De = 200$ and $Pr = 1$. As it is shown in Table 2, a significant agreement between the calculated numerical results and reported numerical results are observed. Therefore the numerical method is reliable while it can predict the developing mixed convection flow in a horizontal curved tube.

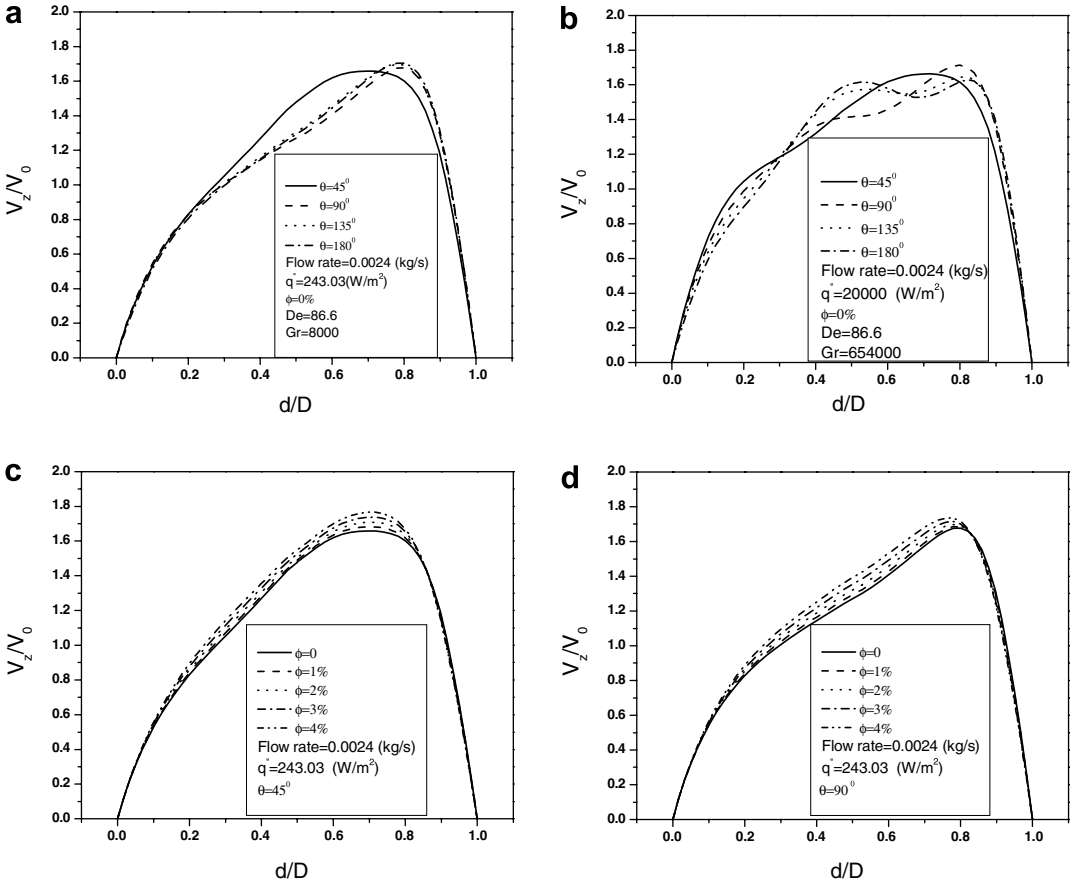

Fig. 8. Axial velocity profiles at horizontal plane.

3. Results and discussion

Numerical simulations are implemented on a wide range of heat flux values as well as flow rates considering five different values of nanoparticles concentrations. However, because of similar behavior and simplicity the results presented here are just for $\dot{m} = 0.0024$, 0.0048 and 0.0071(kg/s) with different values of nanoparticles concentrations (0%, 2%, 4%).

Flow developing and the effects of heat flux value for a given flow rate with two values of nanoparticles concentration at four cross sections are shown in Figs. 4–7. These Figures are oriented in the same manner as shown in Fig. 1 with outer, top, inner and bottom corresponding to $\varphi = 0°$, $\varphi = 90°$, $\varphi = 180°$ and $\varphi = 270°$, respectively.

It can be said that the characteristics of convective heat transfer in curved tubes are strongly dependent on the behavior of the secondary flow. As it is stated in literature, in mixed convection in curved tubes, the secondary flow pattern are influenced by both centrifugal and buoyancy force.

Development of non-dimensional secondary flow ($v_r D/\alpha_{eff}, v_\varphi D/\alpha_{eff}$), dimensionless axial velocity (v_z/v_0) and dimensionless temperature ($(T - T_0)/(T_w - T_b)$) are shown in Figs. 4, 6 and 7, respectively.

Fig. 4 (columns I and III) shows that at low heat flux values, there are two vortices at the bottom and at the top of secondary flow vector. At low heat flux values the impact of buoyancy force is not significant; but due to centrifugal force symmetry is established with respect to the horizontal plane. This figure also shows those vortices are established in the secondary flow vectors at $\theta = 45°$. Because of centrifugal force the flow rate in the core of the tube begins to move to the outer bend, where it is

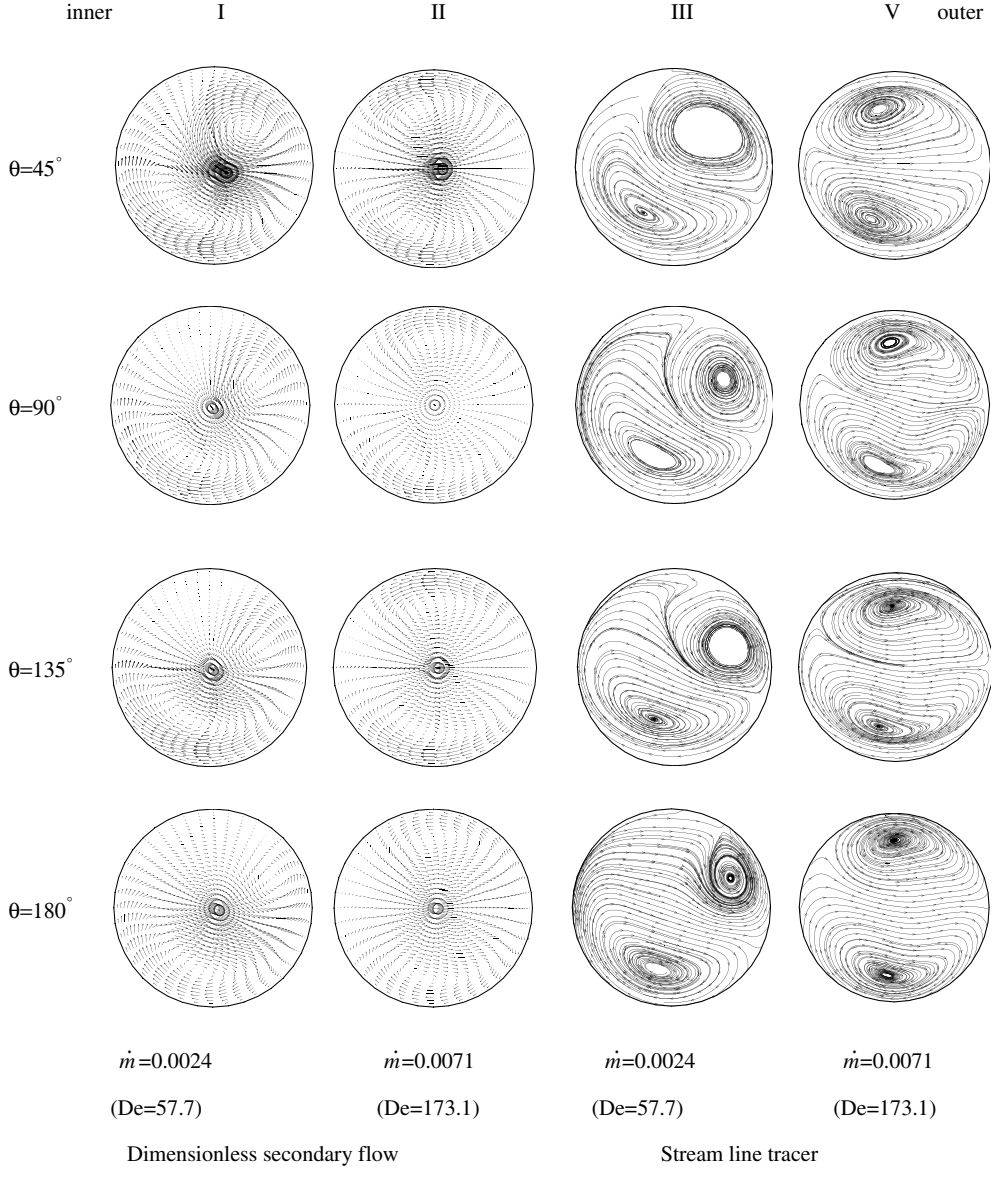

Fig. 9. Effects of flow rate increasing on secondary flow for $\phi = 0.04$, $q'' = 20000$ ($Gr = 285{,}000$).

clearly shown in Fig. 5. Fig. 6 shows that at $\theta = 45°$ centrifugal force causes the medium near the outer bend to be accelerated increasingly. Therefore the maximum axial velocity zone appears at the outer part. This issue causes decreasing the temperature near the outer bend which is illustrated in Fig. 7. Fig. 6 (columns I and III) shows at low heat flux values the axial velocity has been developed at $\theta = 90°$, where it can be seen in Fig. 8(a). Increasing the buoyancy force augments the secondary flow; therefore the axial velocity is developed far away towards the stream direction. So at high heat flux values the axial velocity has been developed at $\theta = 135°$ that is shown in Figs. 6 (columns II and IV) and 8(b).

At high heat flux value, in developing flow; the vortices in the top and bottom zone become smaller towards the stream direction, which is shown in Figs. 4 and 5. Fig. 7 shows by developing in contours of temperature two circular zones corresponding to the vortices will be established. It is interesting to note that circular zones temperature are very low; therefore vortices cause temperature decrease around themselves.

Figs. 4–7 show that increasing heat flux values augments the buoyancy force; hence the symmetry in the vector of secondary flow, contour of axial velocity, streamline tracer and contour of temperature will be distorted. The buoyancy force creates flow in the vertical plane, the distortion of symmetry is due to the interaction between vertical flow and horizontal flow resulted from centrifugal force.

Fig. 6 shows that at a given flow rate increasing nanoparticles concentration causes the augment of axial velocity, while the flow patterns do not change. It occurs in both high and low heat flux values. Based upon Eq. (6) by increasing nanoparticles concentration the density of nanofluid increases. As the effects of centrifugal force on the medium become stronger, the flow will be accelerated that is shown in Fig. 8(c) and (d). Increasing nanoparticles concentration causes the increase of non-dimensional temperature, which is shown in Fig. 7. It is revealed that

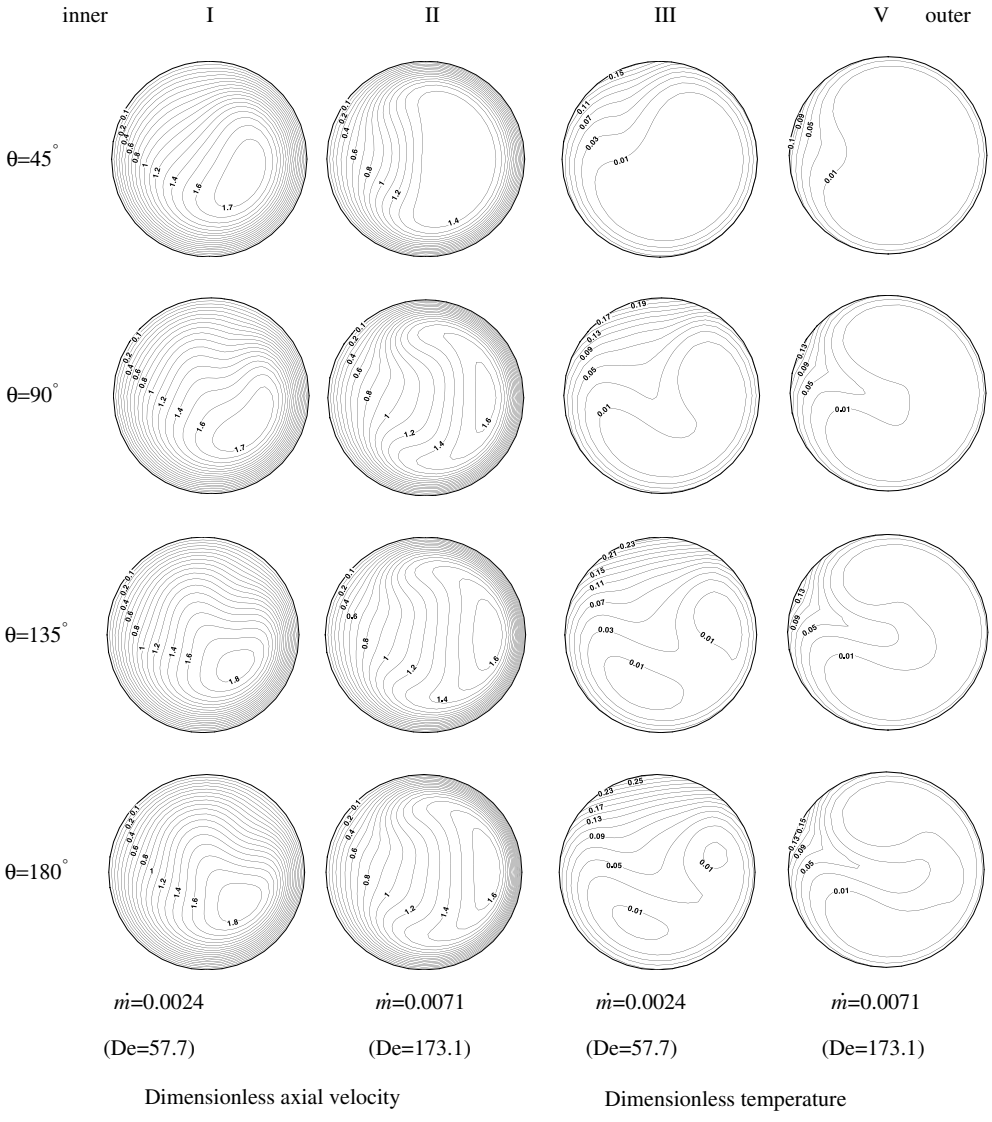

Fig. 10. Effects of flow rate increasing on axial velocity and temperature for $\phi = 0.04$, $q'' = 2000$ ($Gr = 285{,}000$).

increasing nanoparticles concentration augments specific heat and thermal conductivities coefficient. Therefore bulk temperature increases and the difference between bulk temperature and wall temperature becomes low. According to the non-dimensional approach, dimensionless temperature decreases. Increasing nanoparticles concentration does not have any significant impact on the vector of secondary flow. Increasing flow rates increases the centrifugal forces. The effect of increasing centrifugal force is significant at the outer region, where it is dominant at the outer part and symmetry is established at this zone; which is illustrated in Figs. 9 and 10.

Fig. 11 shows developing of local Nusselt number, while the curves for all situations show an initial decrease in the Nusselt number. Initially, the secondary flow causes a few increasing on the boundary layer temperature. After reaching to a minimum, the local Nusselt number beings to increase in the axial direction. This is a sign that the secondary flow resulting from the centrifugal and buoyancy force starts to influence the temperature boundary layer. In a given flow rate an increase in nanoparticles concentration causes a decrease in local Nusselt number. It is acceptable for low as well as high flow rate that are shown in Fig. 11(a) and (b). It can be argued that an increase in nanoparticles concentration causes an increase in heat transfer and effective density. In order to keep flow rate constant the inlet velocity should be decreased. Therefore, the influence of decreasing velocity on Nusselt number is more significant than increasing nanoparticles concentration. At a given heat flux and at a given nanoparticle concentration, increasing flow rates can augment local Nusselt number that is shown in Fig. 11(c). It is interesting that at a given flow rate and at a given nanoparticles concentration, increasing heat flux value initially increases local Nusselt number but after passing $\theta = 65°$ the local Nusselt number decreases. The reason is that, the effects of buoyancy force become stronger towards the stream direction, while the interaction between these effects and the effects of centrifugal force causes the secondary flow becomes weak; resulting local Nusselt number decreases. The developing of the skin friction factor shown in Fig. 12 is similar to the local Nusselt number shown in Fig. 11. Fig. 12(a) and (b) shows that increasing concentration of nanoparticles increases the skin friction factor, which is significant for low and high heat flux values. Fig. 12(c) shows that for a given flow rate and a nanoparticles concentration, heat flux values increment causes a curvy shape of skin friction factor that initially increases but after $\theta = 45°$ it will be decreased. Because along the pipe, the effects of buoyancy force is increased and its interaction with the effect of

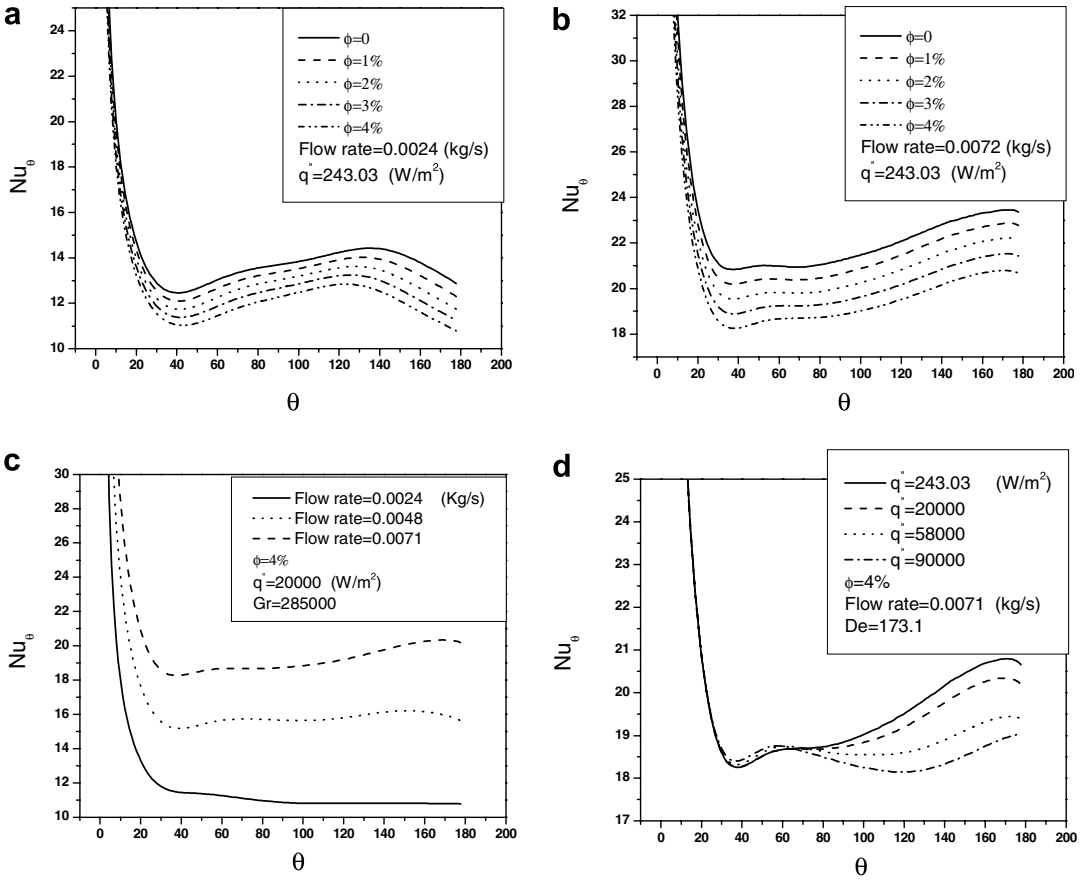

Fig. 11. Effects of volume fraction on the Nusselt number (a, b), effects of mass flow on the Nusselt number (c), effects of heat flux on the Nusselt number (d).

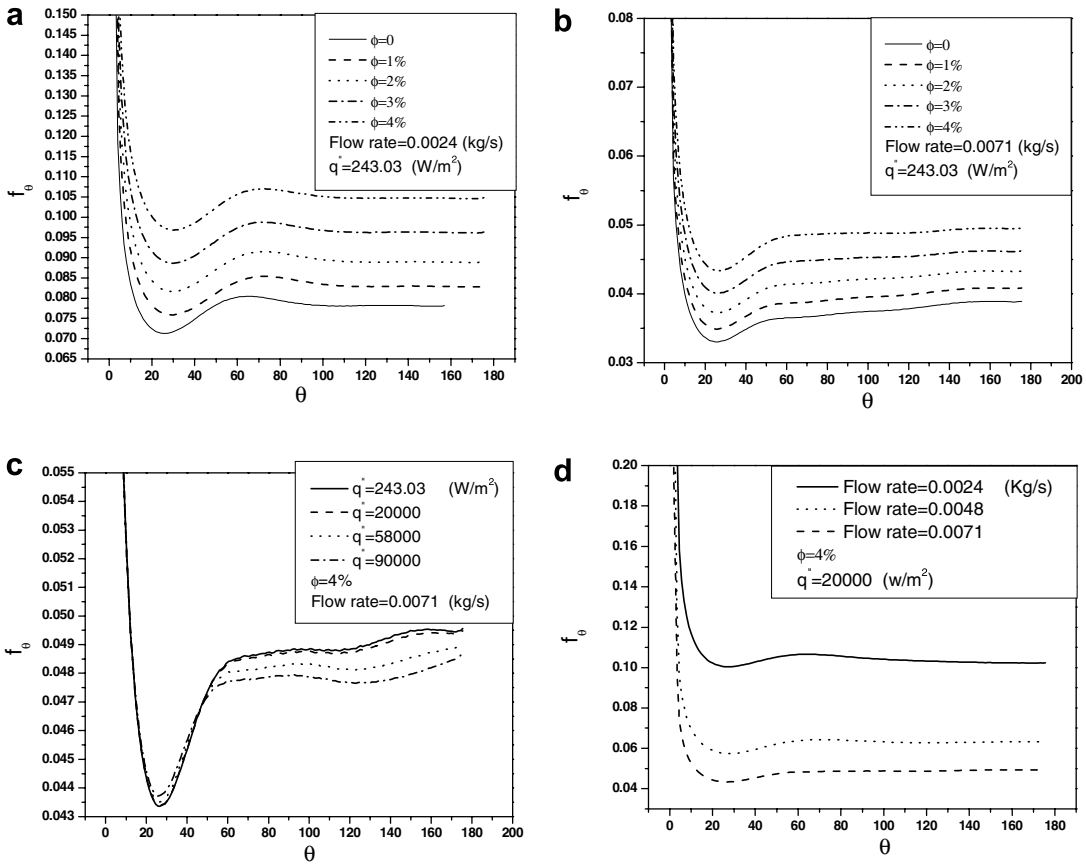

Fig. 12. Effects of volume fraction on the skin friction factor (a, b), effects of heat flux on the skin friction factor (c), effects of mass flow on the skin friction factor (d).

centrifugal force on secondary flow causes a decreasing impact of secondary flow on boundary layer. Increasing flow rate decreases skin friction coefficient that is shown in Fig. 12(d). As skin friction coefficient is proportional to reverse velocity square therefore increasing flow rate causes to decrease skin friction coefficient.

4. Conclusions

Three-dimensional elliptic governing equations is solved to investigate laminar mixed convection of a nanofluid consists of water and Al_2O_3. The effects of buoyancy and heat transfer in a curved tube are studied in this paper. It is shown that for a given flow rate at a given nanoparticles concentration, the increasing in buoyancy force postpone the developing of axial velocity. For a given flow rate, increasing nanoparticles concentration increases axial velocity as well as bulk temperature. In addition, increasing the buoyancy forces augment the Nusselt number and skin friction factor. As soon as the buoyancy force becomes stronger, Nusselt number and skin friction factor are reduced by increasing heat flux. For a given heat flux increasing centrifugal force augments Nusselt number but reduces the skin friction factor. For a given heat flux at a given flow rate, skin friction factor is increased and Nusselt number is reduced by augmenting nanoparticles concentration. Decreasing Nusselt number for a given flow rate by increasing nanoparticles concentration is a crucial issue that reduces the centrifugal force. It is more significant than increasing the buoyancy force in curved tubes.

References

Agrawal, Y., Talbot, L., Gong, K., 1978. Laser anemometer study development in curved circular pipes. J. Fluid Mech. 85 (part 3), 497–518.

Choi, U.S., 1995. Enhancing thermal conductivity of fluid with nanoparticles. In: Singiner, D.A., Wang, H.P. (Eds.), Development and Application of Non-Newronian Flows, FED-vol. 231/MD-vol. 66. The American Society of Mechanical Engineers, New York, NY, pp. 99–105.

Choi, S.U.S., Zhang, Z.G., Yu, W., Lockwood, F.E., Grulke, E.A., 2001. Anomalous thermal conductivity enhancement in nanotube suspension. Appl. Phys. Lett. 79, 2252–2254.

Goering, D.J., Humpherey, J.A.C., Greif, R., 1997. The dual influence of curvature and buoyancy in fully developed tube flows. Int. J. Heat Mass Transfer 49, 2187–2199.

Hamilton, R.L., Crosser, O.K., 1962. Thermal conductivity of heterogeneous two-component system. I & EC Fundamentals 1, 187–191.

Keblinski, P., Phillpot, S.R., Choi, S.U.S., Eastman, J.A., 2002. Mechanisms of heat flow in suspensions of nano-sized particles (nanofluid). Int. J. Heat Mass Transfer 45, 855–863.

Khanafer, K., Vafai, K., Lightstone, M., 2003. Buoyancy-driven heat transfer enhancement in a two-dimensional enclosure utilizing nanofluids. Int. J. Heat Mass Transfer 46, 3639–3653.

Koo, J., Kleinstreuer, C., 2005. Laminar nanofluid flow in microheat-sinks. Int. J. Heat Mass Transfer 48, 2652–2661.

Lee, S., Choi, S.U.S., Li, S., Eastman, J.A., 1999. Measuring thermal conductivity of fluids containing oxide nanoparticles. ASME J. Heat Transfer 121, 280–288.

Liu, K.V., Choi, S.U.S., Kasza, K.E., 1988. Measurement of pressure drop and heat transfer in turbulent pipe flows of particulate slurries, Argonne National Laboratory Report, ANL-88-15.

Maiga, S.E.B., Nguyen, C.T., Galanis, N., Roy, G., 2004. Heat transfer behaviors of nanofluids in a uniformly heated tube. Superlattices Microstruct. 35, 543–557.

Masuda, H., Ebata, A., Teramae, K., Hishinuma, N., 1993. Alteration of thermal conductivity and viscosity of liquid by dispersing ultra-fine particles (dispersions of -Al_2O_3, SiO_2, and TiO_2 ultra-fine particles). Netsu Bussei (Japan) 4, 227–233.

Maxwell, J.C., 1873. Electricity and Magnetism. Clarendon press, Oxford, Uk.

Maxwell, J.C., 1904. A Treatise on Electricity and Magnetism, second ed. Oxford University Press, Cambridge, pp. 435–441.

Pak, B.C., Cho, Y.I., 1998. Hydrodynamic and heat transfer study of dispersed fluids with submicron metallic oxide particles. Exp. Heat Transfer 11, 151–170.

Palm, S.J., Roy, G., Nguyen, C.T., 2006. Heat transfer enhancement with the use of nanofluids in radial flow cooling systems considering temperature dependent properties. Appl. Thermal Eng. 26, 2209–2218.

Roy, G., Nguyen, C.T., Lajoie, P.R., 2004. Numerical investigation of laminar flow and heat transfer in a radial flow cooling system with the use of nanofluids. Superlattices Microstruct. 35, 497–511.

Wang, X., Xu, X., Choi, S.U.S., 1999. Thermal conductivity of nanoparticle–fluid mixture. J. Thermophys. Heat Transfer 13, 474–480.

Xuan, Y., Li, Q., 2000. Heat transfer enhancement of nanofluids. Int. J. Heat Fluid Flow 21, 58–64.

Xuan, Y.M., Li, Q., 2003. Investigation on convective heat transfer and flow features of nanofluids. J. Heat Transfer 125, 151–155.

Xuan, Y., Roetzel, W., 2000. Conceptions for heat transfer correlations of nanofluids. Int. J. Heat Mass Transfer 43, 3701–3707.

Xuan, Y.M., Li, Q., Hu, W., 2003. Aggregation structure and thermal conducting of nanofluids. AIChE J. 49, 1038–1043.

Xue, Q.Z., 2003. Model for effective thermal conductivity of nanofluids. Phys. Lett. A 307, 313–317.

Yang, R., Chang, S.F., 1994. Combined free and forced convection for developed flow in curved pipe with finite curvature ratio. Int. J. Heat Fluid Flow 15, 470–476.

Yang, Y., Zhang, Z.G., Grulke, E.A., Anderson, W.B., Wu, G., 2005. Heat transfer properties of nanoparticle-in-fluid dispersions (nanofluids) in laminar flow. Int. J. Heat Mass Transfer 48, 1106–1116.

Zhang, X., Gu, H., Fujii, M., 2006. Effective thermal conductivity and thermal diffusivity of nanofluids containing spherical and cylindrical nanoparticles. J. Appl. Phys. 100 (4), 044325–044330.

Zheng, B., Lin, C.X., Ebadian, M.A., 2003. Combined turbulent forced convection and thermal radiation in a curved pipe with uniform wall temperature. Numer. Heat Transfer 44 (part A), 149–167.